

Structural characterisation of CN_x thin films deposited by pulsed laser ablation

Gareth M. Fuge, Christopher J. Rennick, Seán R.J. Pearce, Paul W. May, Michael N.R. Ashfold*

School of Chemistry, University of Bristol, Bristol BS8 1TS, UK

Abstract

Carbon nitride (CN_x) film growth by 193 nm pulsed laser ablation of graphite in a low pressure of N_2 has been investigated both by studying optical emission from the plume and by analyses of the composition, structure and bonding of material deposited at a range of substrate temperatures. Spectral analysis of the emission reveals the presence of C^+ ions, C atoms, C_2 and CN radicals and N_2^+ molecular ions within the ablation plume travelling towards the substrate. Films deposited at low substrate temperature (T_{sub}) are amorphous, with an N/C ratio of ~ 20 at.%. Raman analysis shows CN_x films grown at higher T_{sub} to be increasingly nanocrystalline, but thinner, and suggests that N inclusion encourages nanocrystallite formation. X-ray photoelectron spectroscopy reveals that CN_x films grown at higher T_{sub} also have a reduced overall N content. The observations have been rationalised by assuming an increased propensity for sputtering or desorption of more labile CN species from the growing film surface at higher T_{sub} , resulting in a higher fraction of C–C bonding—most probably in the form of graphitic nanocrystallites embedded in an amorphous matrix.

© 2003 Elsevier Science B.V. All rights reserved.

Keywords: Carbon nitride; Pulsed laser deposition; Optical emission; Composition; Structure

1. Introduction

Theoretical predictions that crystalline $\beta\text{-C}_3\text{N}_4$ might have a higher hardness than diamond [1] have served to inspire numerous attempts at carbon nitride (CN_x) film deposition [2]. Techniques employed in this quest include hot filament assisted chemical vapour deposition (CVD) [3], pulsed laser ablation (PLA) of graphite in a background pressure of nitrogen [4–8], magnetron and ion beam sputtering [9,10], N^+ ion implantation into amorphous carbon (a-C) films [11], and filtered cathodic arc methods [12–14]. Several of the pulsed laser deposition (PLD) studies have investigated the potential benefits of separate activation of the nitrogen using, for example, radio frequency (RF) or DC glow discharges to increase the N/C ratio in the deposited films [7,15–17]. Substrate temperature, T_{sub} , is recognised as another key parameter influencing the CN_x film composition and the bonding structure within the film. CN_x films deposited at higher substrate temperatures have been reported to exhibit lower N/C ratios, a more graphitic

structure, increased hardness and much improved room temperature electrical conductivity [4,7,18,19]. Enhanced surface atom mobility, and an increased tendency for rupture of weak $\sigma(\text{C}-\text{N})$ bonds and the relaxation of sub-planted C atoms have all been advanced as potential explanations for these observations.

The present work describes further careful studies of CN_x film growth, based on ArF (193 nm) laser ablation of a graphite target in the presence of nitrogen, with and without a DC glow discharge, on both Si and NaCl substrates, as a function of T_{sub} in the range 25–400 °C. The resulting CN_x films have been investigated by Fourier transform infrared (FTIR), laser Raman and X-ray photoelectron spectroscopy (XPS), and by secondary ion mass spectrometry (SIMS) and compared, where appropriate, with films grown under otherwise equivalent conditions in Ar rather than N_2 . Compositional and structural changes that accompany changes in T_{sub} are identified and discussed.

2. Experimental

The experimental apparatus and much of the procedure has been described previously in the context of the

*Corresponding author. Tel.: +44-117-928-8312; fax: +44-117-925-0612.

E-mail address: mike.ashfold@bris.ac.uk (M.N.R. Ashfold).

PLD of amorphous carbon films [20,21]. Briefly, the output of an ArF excimer laser (Lambda-Physik, Compex 201) operating at 193 nm was steered by two highly reflective mirrors through an aperture and a fused silica lens (200 mm focal length) onto a high-purity graphite target. This target is mounted on a rotating stage, in a stainless steel ablation chamber that can be evacuated to a base pressure of $<10^{-6}$ torr by a 100 mm turbomolecular pump, backed by a two-stage rotary pump. The focal area on the target is estimated to be ~ 0.4 mm². During a deposition run, N₂ (or Ar) was admitted through a mass-flow controller (5 sccm flow rate) and the pumping throttled to maintain a pressure of 20 mtorr. At these pressures it was possible to strike and maintain a DC glow discharge between the grounded target and a biased (+1.5 kV), 27-mm-diameter stainless steel ring electrode positioned at $d \sim 30$ mm along the target surface normal. Films were deposited on both freshly cleaved NaCl and n-type single crystal (100) Si substrates (~ 1 cm² in area). These were mounted on the target surface normal, 80 mm distant from the focal spot, on a purpose designed holder positioned immediately in front of a compact 15 W light bulb heater which enabled deposition at any user selected $T_{\text{sub}} \leq 400$ °C.

Fluorescence accompanying the ablation plume was investigated by optical emission spectroscopy (OES). As previously [20,21], light emanating from a ~ 2 mm diameter viewing column orthogonal to the surface normal was focused onto the end of a quartz fibre-optic bundle mounted on a translation stage, and directed into an Oriel 12.5 cm monochromator equipped with a 600 lines/mm ruled grating and a UV extended Instaspec IV CCD array detector. Signal accumulation over 50–100 laser shots suffices to provide low resolution (~ 1 nm) wavelength resolved spectra of the emission, at any user selected distance along the surface normal.

The deposited films were analysed by FTIR and Raman (Renishaw 2000 system equipped with 325, 514.5 and 785 nm excitation lasers) spectroscopy, and by XPS using a Fisons Instruments VG Escascope equipped with a MgK α (1253.6 eV) X-ray source and an analyser energy resolution of ~ 0.9 eV. Absolute N/C ratios (and insight into the nature and extent of subsequent film oxidation) were determined by comparing the respective 1s peak areas, A_x , weighted by the appropriate atomic sensitivity factors (i.e. $N/C/O = A_C/0.25:A_N/0.42:A_O/0.66$). Selected films were also analysed by secondary ion mass spectrometry (SIMS) in an attempt to gain further insight into the oxidation of CN_x films.

3. Results and discussion

Fig. 1 shows a spectrum of the wavelength resolved emission in the range 300–600 nm, recorded at $d=2$ mm, when ablating graphite at 193 nm in 20 mtorr of

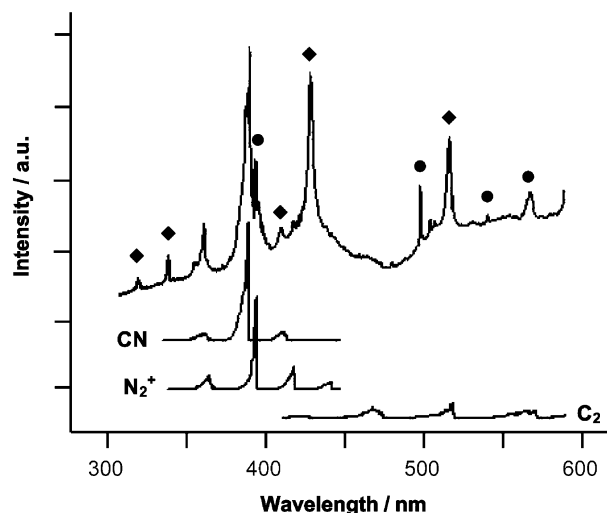


Fig. 1. Wavelength dispersed spectrum of the emission accompanying 193 nm PLA of graphite in 20 mtorr N₂, using an incident fluence $F \sim 10$ J cm⁻², measured at $d=2$ mm. The spectrum has not been corrected for the wavelength dependence of the transmission of the quartz fibre bundle, the grating reflectivity or the efficiency of the CCD array detector; the overall detector sensitivity is $\sim 4 \times$ higher at 600 nm than at 280 nm. Bands associated with the CN($B^2\Sigma^+ \rightarrow X^2\Sigma^+$), N₂⁺($B^2\Sigma_u^+ \rightarrow X^2\Sigma_g^+$) and C₂($d^3\Pi_u \rightarrow a^3\Pi_g$) transitions are indicated by the underlying spectral simulations [30]; these illustrative band contours have been produced using literature values of all relevant spectroscopic constants [31] and excited state population distributions characterised by a rovibrational temperature of 3000 K. All other features may be assigned to electronically excited C atoms (indicated ●) and C⁺ ions (◆).

background N₂ at an incident fluence $F \sim 15$ J cm⁻². Emissions attributable to electronically excited C atoms, C⁺ ions and the diatomic species C₂, CN and N₂⁺ are all clearly discernible, even in the absence of the secondary DC discharge. The analogous spectra recorded with the DC glow discharge present show a marked increase in the relative intensities of the CN and N₂⁺ emissions, whereas neither of these carriers are present in the corresponding spectra recorded with Ar rather than N₂ as the background gas. Such observations accord with previous studies of the plume emission accompanying ultraviolet laser ablation of graphite in N₂ (e.g. at 248 nm [8] and at 308 nm [22]) and confirm CN bond formation in the gas phase, even without assisted activation of the background gas. The various emissions, and their spatial extent, can be understood in terms of a sequence of steps initiated by ejection of energetic C atoms and ions and subsequent ion-electron recombination [21], heating of the resulting plasma ball by inverse Brehmstrahlung absorption, ionisation of the background gas in this region (largely N₂) and subsequent collisions leading to the observed CN and C₂ emitters.

Illustrative Raman spectra (recorded using an excitation wavelength of 514.5 nm) of films grown by PLA of graphite in 20 mtorr background pressures of, respec-

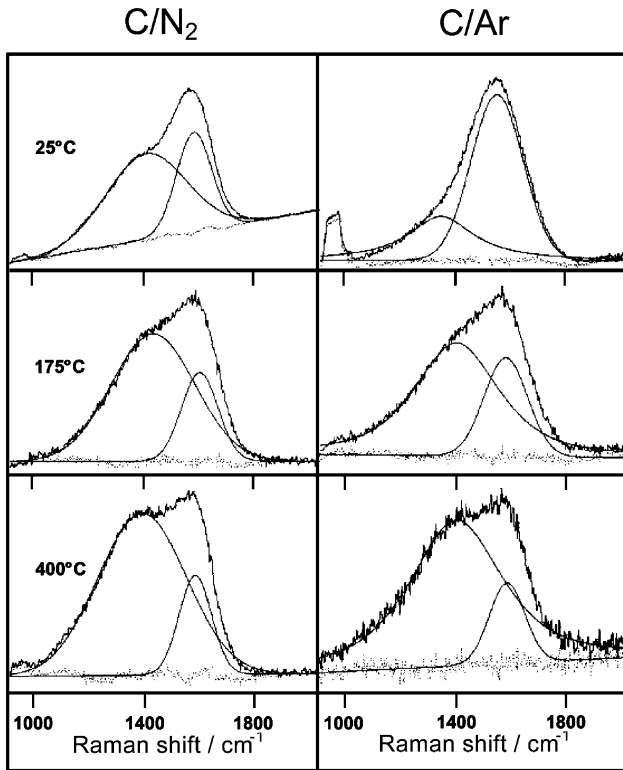


Fig. 2. Raman spectra (514.5 nm excitation wavelength) of CN_x films grown on Si by PLA of graphite in 20 mtorr background pressures of N_2 (left hand column) and Ar (right hand column), at $T_{sub} = 25, 175$ and 400 °C. Each is fitted in terms of two independent Gaussian functions (solid curves) after subtracting a linear contribution for background fluorescence. The dashed line at $y \sim 0$ is a plot of the residuals of the fit.

tively, nitrogen (left hand column) and Ar (right hand column), at three different substrate temperatures are shown in Fig. 2. The displayed spectra span the range of Stokes shifts $1000\text{--}2000\text{ cm}^{-1}$ only; wider scans also show a broad second order phonon band at $\sim 3000\text{ cm}^{-1}$ in each case, and the $C\equiv N$ peak at $\sim 2225\text{ cm}^{-1}$ is also clearly evident in the CN_x films, particularly those grown at low T_{sub} . We attribute the evident decrease in signal to noise ratio of the spectra of films grown at higher T_{sub} to increasing film opacity (at 514.5 nm). This being so, the observed near constant intensity of the second-order Si peak at $\sim 950\text{ cm}^{-1}$ implies that CN_x films deposited at higher T_{sub} are thinner. Each spectrum was deconvoluted as illustrated, using Gaussian functions, into contributions associated with the D and G vibrational modes of graphite. Ferrari and Robertson [23] have proposed a model relating the variation of parameters derived by fitting such Raman spectra and the structure of disordered carbon films. Quantities of interest include the wavenumbers of the G and D band maxima, G_{max} and D_{max} at $\sim 1570\text{ cm}^{-1}$ and 1380 cm^{-1} respectively and the ratio of the peak intensities of the deconvoluted D and G bands, $I(D)/I(G)$.

Fig. 3 illustrates how each of these quantities varies with T_{sub} , for films grown in 20 mtorr of both Ar and N_2 . In both cases, G_{max} is seen to shift to higher wavenumber with increasing T_{sub} ; D_{max} also shifts to higher wavenumber as T_{sub} is increased in the case of the pure carbon films (i.e. films grown in Ar), but remains relatively constant for films grown in N_2 . The $I(D)/I(G)$ ratio is also seen to increase with T_{sub} in both cases, but shows a higher room temperature value and appears to maximise at a slightly lower T_{sub} when using N_2 as background gas. For carbon films, at least, the trends in G_{max} and $I(D)/I(G)$ can be understood in terms of films that are best described as amorphous carbon (a-C) at low T_{sub} but which tend towards nanocrystalline graphite (nc-G) at higher T_{sub} [23]. Nitrogen incorporation can be expected to introduce additional complexity, not least because any Raman features associated with C–N and C=N stretches will fall within the wavenumber range covered by the G and D bands. Given the rather modest level of N incorporation deduced below, however, we elect to extend this discussion of film structure and bonding to include the deposited CN_x films also. Once again, the observed increase in both G_{max} and $I(D)/I(G)$ with increasing T_{sub} is interpreted in terms of a shift from amorphous to nanocrystalline film growth. In the case of CN_x films,

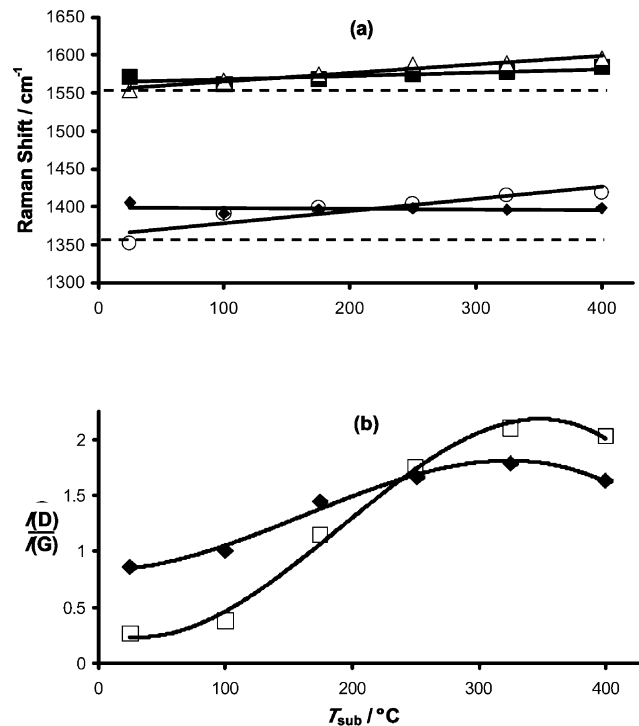


Fig. 3. Plots showing the variation of (a) G_{max} and D_{max} , and (b) $I(D)/I(G)$ with T_{sub} for films grown by PLA of graphite in 20 mtorr of N_2 (closed symbols) and Ar (open symbols). The dashed horizontal lines in (a) indicate the corresponding peak positions for polycrystalline graphite.

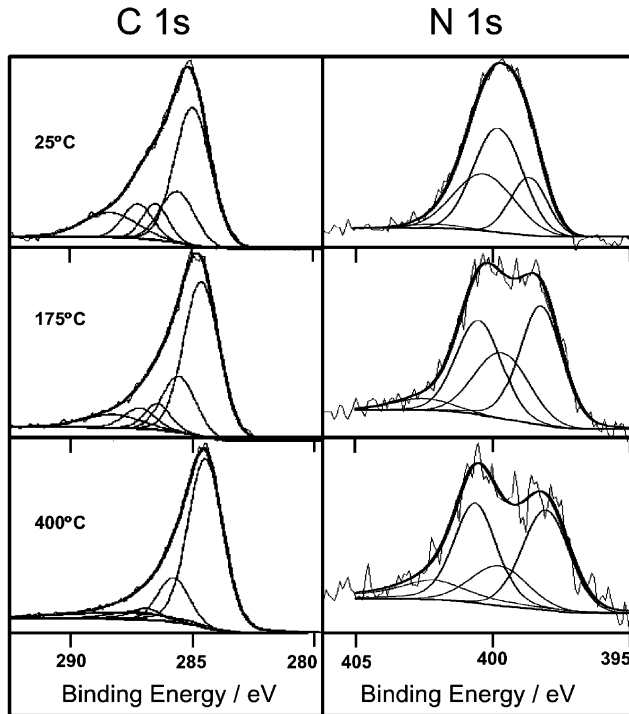


Fig. 4. C(1s) and N(1s) XPS spectra of CN_x films deposited via DC plasma assisted PLA of graphite in N_2 , at $T_{\text{sub}}=25, 175$ and 400°C . Each has been deconvoluted by fitting to four [in the case of N(1s)] or five [for the C(1s) peak] Voigt lineshape functions as discussed in the text.

the room temperature $I(\text{D})/I(\text{G})$ ratio is higher than for carbon films deposited in an Ar background. The ratio also appears to peak at a slightly lower T_{sub} value. Such results accord well with others reported recently for CN_x films grown by DC plasma assisted 248 nm PLA of graphite in N_2 [7]. All of these trends may be rationalised by assuming that N incorporation relaxes some of the constraints associated with nanocrystalline domain formation, allowing growth of larger crystallites at lower T_{sub} .

C(1s) and N(1s) XPS binding energy spectra of films deposited via DC plasma assisted PLA of graphite in N_2 , at three different T_{sub} values, which were then left to stand in air for >1 month, are shown in Fig. 4. The low energy edge of both peaks are seen to shift to progressively lower energies in the case of films deposited at higher T_{sub} . This observation is attributed to reduced surface charging, consistent with the reported improvement in electrical conductivity (and more graphitic nature) of CN_x films deposited at higher T_{sub} [4]. Comparison of the relative areas of these peaks, weighted by the appropriate atomic sensitivity factors, gives an N/C ratio of ~ 20 at.% in films deposited at room temperature, which declines with increasing T_{sub} as shown in Fig. 5a. Both the absolute value of this room temperature N/C ratio, and the measured temperature

dependence accords with that found in several other studies of CN_x film growth, using both PLD and filtered cathodic arc methods [4,7,8,13]. The trend has been explained by assuming an increased atomic mobility within the film at higher T_{sub} , that both encourages the escape of gaseous species like N_2 and discourages the incorporation of more volatile adsorbate species like CN [24]. XPS also reveals the presence of oxygen [via the O(1s) peak at ~ 399.2 eV] in the CN_x films. This impurity is present at the $\sim 2\%$ level in films analysed within a few hours of deposition, but can be $>10\%$ in films left exposed to air for a month. Such progressive

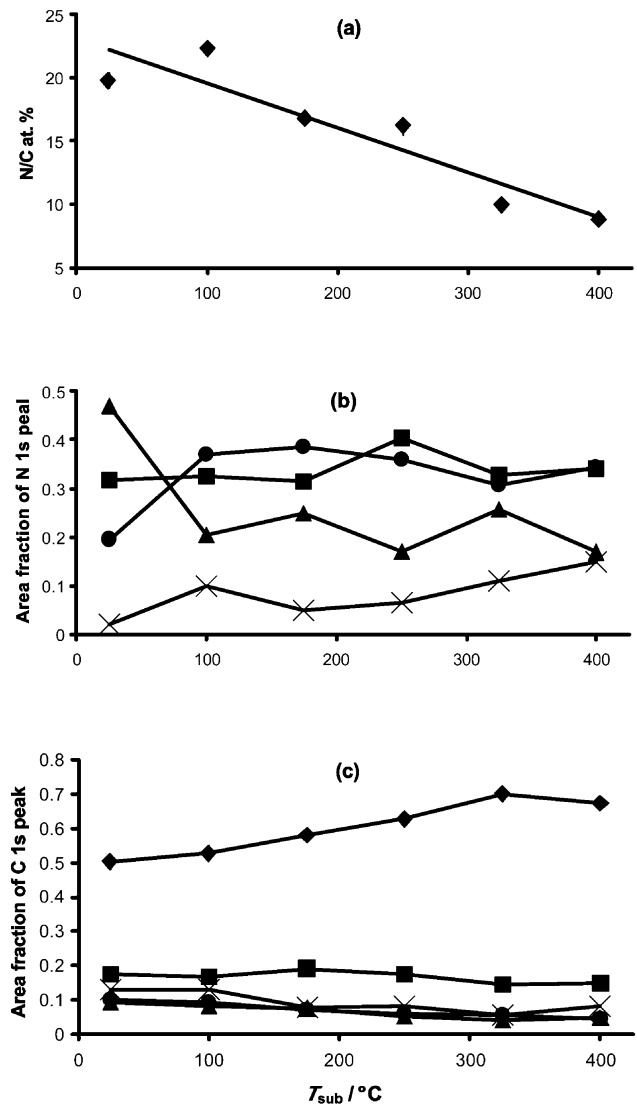


Fig. 5. Plots showing the T_{sub} dependencies of (a) the N/C atomic ratio of CN_x films deposited via DC plasma assisted PLA of graphite in N_2 , (b) the relative areas of the Voigt functions used to fit the N(1s) XPS peak [Key: 398.5 eV (\bullet), 399.6 eV (\blacktriangle), 400.2 eV (\blacksquare) and 402.5 eV (\times)], (c) the relative areas of the Voigt functions used to fit the C(1s) XPS peak [Key: 284.6 eV (\blacklozenge), 285.5 eV (\blacksquare), 286.6 eV (\blacktriangle), 287.0 eV (\bullet) and 288.5 eV (\times)].

oxidation upon exposure to air has been discerned and discussed in some detail in previous IR absorption studies of hydrogenated CN_x films [25]. The extent of this long-time O contamination appears to scale with T_{sub} —suggesting that the ease of atmospheric oxidation is sensitive to the film content and structure. Of course, XPS is a notoriously surface sensitive technique so, in an effort to gain further insight into the film oxidation process, composition depth profiles of selected films were undertaken using Ga ion bombardment and SIMS, in negative ion mode. C^- , C_2^- and CN^- anions showed prominently, with ratios that were essentially independent of depth. O^- anions were also clearly identifiable in the SIMS analysis, with relative yields that increase with depth and maximise at the CN_x film/Si interface.

The evident breadth and asymmetry of the C(1s) and N(1s) XPS peaks shown in Fig. 4 indicates the presence of different bonding types within the film, the relative importances of which vary with T_{sub} . Unfortunately, the literature contains contradictory interpretations of the sub-structure within these peaks. In the case of the N(1s) peak there appears to be reasonable consensus that N atoms bonded to sp^3 hybridised C atoms show a lower binding energy (~ 398.5 eV) than those bonded to sp^2 hybridised carbons [henceforth represented as N–C(sp^2)], at ~ 400.2 eV [2,26]. Signal observed at yet higher binding energy (~ 402.5 eV) is traditionally ascribed to N atoms bonded to O (or another N) atom. Deconvolution of the N(1s) XPS peaks measured at all T_{sub} values in terms of three such basis lineshapes gave reasonable fits, but each was found to be significantly improved by inclusion of a fourth peak centred at a binding energy of ~ 399.6 eV. Given previous discussions, some have attributed this contribution to N atoms bonded to sp hybridised C atoms (i.e. $-\text{C}\equiv\text{N}$ moieties) [2,27]. The deconvolution of the N(1s) peaks shown in Fig. 4 involves fitting to all four basis lineshapes. Their deduced variation with T_{sub} , summarised in Fig. 5b, indicates a marked decrease in N–C(sp) bonding and a rise in the N–O contribution in films grown at elevated T_{sub} . This conclusion is little changed if the measured peak is subjected to the more traditional three-lineshape deconvolution. Most of the peak area we attribute to N–C(sp) bonding is now collected within the N–C(sp^2) lineshape and it is this unsaturated contribution that is deduced to decline with increasing T_{sub} .

The deconvolution of C(1s) XPS spectra of CN_x films is even less secure [2,5–7,28,29]. N inclusion causes the C(1s) peak to broaden, asymmetrically, to higher binding energies. Signal at low energies (centred at ~ 284.6 eV) is generally associated with C–C(sp^2) graphitic bonding. Given the variety of possible bonding configurations, Le Normand et al. [28] have argued that it is inappropriate to try and assign components appearing at higher binding energies to specific C–C or C–N bonding environments, but many others have proceeded

to attribute signal centred at ~ 285.5 eV and ~ 286.9 eV to C(sp^2)–N and C(sp^3)–N bonding, respectively. Cheng et al. [7] suggest further partitioning of the latter signal into components specifically associated with C(sp) and C(sp^3) atoms bonded to N while, as with the N(1s) peak, several authors propose that C bonded to O atoms will be shifted to highest binding energy (~ 289 eV). The deconvolutions of the C(1s) peaks shown in Fig. 4 follow these attributions but, as Fig. 5c shows, only the signal attributed to C–C(sp^2) bonding shows any distinctive variation—increasing with T_{sub} while all other components show a systematic decline. Both these trends, and the T_{sub} dependence of the N(1s) signal, are in broad accord with results reported recently following 248 nm PLA of graphite in low pressures of N_2 activated with a DC glow discharge [7].

4. Conclusions

This paper presents analyses of the optical emission accompanying 193 nm PLA of graphite in a low pressure of N_2 and of the way the composition, structure and bonding of the resulting CN_x films varies with substrate temperature. OES demonstrates the presence of C^+ ions, C atoms, C_2 and CN radicals and N_2^+ molecular ions within the ablation plume that propagates towards the substrate. Films deposited at low T_{sub} are amorphous, with an N/C ratio of ~ 20 at.%. Raman analysis shows CN_x films grown at higher T_{sub} to be increasingly nanocrystalline, but thinner, and suggests that N inclusion encourages nanocrystallite formation. However, XPS analysis shows that CN_x films grown at higher T_{sub} have a reduced overall N content. Growth at higher substrate temperatures appears to mitigate against incorporation of N atoms adjacent to one or more unsaturated C atoms—perhaps reflecting an increased propensity for sputtering or desorption of more labile CN species from the growing film surface at higher T_{sub} —and to result in a higher fraction of C–C bonding—most probably in the form of graphitic nanocrystallites embedded in an amorphous matrix. XPS and SIMS analysis indicate that all CN_x films produced in this work oxidise progressively with time, especially those deposited at high T_{sub} , and that O incorporation invokes bonding to primarily N rather than C atoms.

Acknowledgments

The authors are grateful to the EPSRC for financial support in the form of equipment grants, a Senior Research Fellowship (MNRA) and studentships (GMF and SRJP), to the staff of the Interface Analysis Centre at the University of Bristol, and to colleagues K.N. Rosser and Dr S.J. Henley for their many and varied contributions to this work.

References

- [1] A.Y. Liu, M.L. Cohen, *Phys. Rev. B* 41 (1990) 10727.
- [2] S.F. Muhl, J.M. Mendez, *Diamond Relat. Mater.* 8 (1999) 1809, and references therein.
- [3] Y. Zhang, Z. Zhou, H. Li, *Appl. Phys. Lett.* 68 (1996) 634.
- [4] C.W. Ong, X.-A. Zhao, Y.C. Tsang, C.L. Choy, P.W. Chan, *Thin Solid Films* 280 (1996) 1.
- [5] J.P. Zhao, Z.Y. Chen, T. Yano, T. Ooie, M. Yoneda, *J. Appl. Phys.* 89 (2001) 1580.
- [6] E. Gyorgy, V. Nelea, I.N. Mihailescu, A. Perrone, H. Pelletier, A. Cornet, et al., *Thin Solid Films* 388 (2001) 93.
- [7] Y.H. Cheng, X.L. Qiao, J.G. Chen, Y.P. Wu, C.S. Xie, Y.Q. Wang, et al., *Diamond Relat. Mater.* 11 (2002) 1511.
- [8] A.A. Voevodin, J.G. Jones, J.S. Zabinski, L. Huttman, *J. Appl. Phys.* 92 (2002) 724.
- [9] T.R. Lu, C.T. Kuo, J.R. Yang, L.C. Chen, K.H. Chen, T.M. Chen, *Surf. Coating Technol.* 115 (1999) 116.
- [10] N. Hellgren, K. Macak, E. Broitman, L. Hultman, J.-E. Sundgren, *J. Appl. Phys.* 88 (2001) 524.
- [11] D.-H. Lee, H. Lee, B. Park, D.B. Poker, L. Riester, *Appl. Phys. Lett.* 70 (1997) 3104.
- [12] J.H. Kaufman, S. Metin, D.D. Saperstein, *Phys. Rev. B* 39 (1989) 13053.
- [13] C. Spaeth, M. Kühn, U. Kreissig, F. Richter, *Diamond Relat. Mater.* 6 (1997) 626.
- [14] S.E. Rodil, W.I. Milne, J. Robertson, L.M. Brown, *Appl. Phys. Lett.* 77 (2000) 1458.
- [15] P. Merel, M. Chaker, M. Tabbal, M. Moisan, *Appl. Phys. Lett.* 71 (1997) 3814.
- [16] J.T. Hu, P. Yang, C.M. Lieber, *Phys. Rev. B* 57 (1998) R3185, and references therein.
- [17] Y. Aoi, K. Ono, E. Kamijo, *J. Appl. Phys.* 86 (1999) 2318.
- [18] X.-A. Zhao, C.W. Ong, Y.C. Tsang, K.F. Chan, C.L. Choy, P.W. Chan, et al., *Thin Solid Films* 322 (1998) 245.
- [19] M.E. Ramsey, E. Poindexter, J.S. Pelt, J. Marin, S.M. Durbin, *Thin Solid Films* 360 (2000) 82.
- [20] R.J. Lade, F. Claeysens, K.N. Rosser, M.N.R. Ashfold, *Appl. Phys. A: Mater. Sci. Process.* 69 (1999) S935.
- [21] F. Claeysens, R.J. Lade, K.N. Rosser, M.N.R. Ashfold, *J. Appl. Phys.* 89 (2001) 697.
- [22] S. Acquaviva, M.L. De Giorgi, *J. Phys. B., At. Mol. and Opt. Phys.* 35 (2002) 795, and references therein.
- [23] A.C. Ferrari, J. Robertson, *Phys. Rev. B* 61 (2000) 14095, and references therein.
- [24] T. Sebald, R. Kaltofen, G. Weise, *Surf. Coat. Technol.* 98 (1998) 1280.
- [25] F. Alvarez, N.M. Victoria, P. Hammer, F.L. Freire Jr., M.C. dos Santos, *Appl. Phys. Lett.* 73 (1998) 1065.
- [26] N. Hellgren, M.P. Johansson, E. Broitman, L. Hultman, J.-E. Sundgren, *Phys. Rev. B* 59 (1999) 5162.
- [27] N. Hellgren, J. Guo, C. Sæthe, A. Agui, J. Nordgren, Y. Luo, et al., *Appl. Phys. Lett.* 79 (2001) 4348.
- [28] F. Le Normand, J. Hommet, T. Szörenyi, C. Fuchs, E. Fogarassy, *Phys. Rev. B* 64 (2001) 235416.
- [29] C. Jama, A. Al khawwam, A.-S. Loir, P. Goudmand, O. Dessaux, L. Gengembre, et al., *Surf. Interface Anal.* 31 (2001) 815.
- [30] M.E. Green, C.M. Western, *J. Chem. Phys.* 104 (1996) 848, A summary of the program and the Hamiltonian used is given on the PGOPHER spectral simulation program written by C.M. Western.
- [31] K.P. Huber, G. Herzberg, *Molecular spectra and molecular structure IV, Constants of Diatomic Molecules*, Van Nostrand, New York, 1979, and references therein.